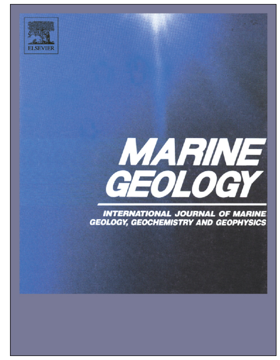

Sedimentary records of coastal storm surges: Evidence of the 1953 North Sea event

Graeme T. Swindles, Jennifer M. Galloway, Andrew L. Macumber, Ian Croudace, Andy R. Emery, Clare Woulds, Mark D. Bateman, Lauren Parry, Julie M. Jones, Katherine Selby, Greg T. Rushby, Andy J. Baird, Sarah A. Woodroffe, Natasha L.M. Barlow

PII: S0025-3227(18)30076-8
DOI: doi:10.1016/j.margeo.2018.06.013
Reference: MARGO 5812

To appear in: *Marine Geology*

Received date: 27 March 2018
Revised date: 19 June 2018
Accepted date: 22 June 2018

Please cite this article as: Graeme T. Swindles, Jennifer M. Galloway, Andrew L. Macumber, Ian Croudace, Andy R. Emery, Clare Woulds, Mark D. Bateman, Lauren Parry, Julie M. Jones, Katherine Selby, Greg T. Rushby, Andy J. Baird, Sarah A. Woodroffe, Natasha L.M. Barlow , Sedimentary records of coastal storm surges: Evidence of the 1953 North Sea event. Margo (2018), doi:10.1016/j.margeo.2018.06.013

Sedimentary records of coastal storm surges: evidence of the 1953 North Sea event

Graeme T. Swindles[1*], Jennifer M. Galloway[2], Andrew L. Macumber[3], Ian Croudace[4], Andy R. Emery[5], Clare Woulds[1], Mark D. Bateman[6], Lauren Parry[7], Julie M. Jones[6], Katherine Selby[8], Greg T. Rushby[6], Andy J. Baird[1], Sarah A. Woodroffe[9] and Natasha L.M. Barlow[5]

1. *School of Geography, University of Leeds, LS2 9JT, UK*
2. *Natural Resources Canada/Ressources naturelles Canada, Geological Survey of Canada/Commission géologique du Canada, Calgary, Alberta T2L 2A7, Canada*
3. *School of Natural and Built Environment, Queen's University Belfast, UK*
4. *GAU-Radioanalytical, University of Southampton, National Oceanography Centre Southampton, SO14 3ZH, UK*
5. *School of Earth and Environment, University of Leeds, LS2 9JT, UK*
6. *Department of Geography, The University of Sheffield, S10 2TN, UK*
7. *School of Interdisciplinary Studies, University of Glasgow, DG1 4ZL, UK*
8. *Environment Department, University of York, YO10 5NG, UK*
9. *Department of Geography, Durham University, DH1 3LE, UK*

*Email: g.t.swindles@leeds.ac.uk

Keywords: Storm surge; 1953 storm; North Sea; Salt marsh; ^{137}Cs dating, Core scanning X-ray fluorescence; sedimentology

Manuscript for *Marine Geology*

Abstract

The expression of storm events in the geological record is poorly understood; therefore, stratigraphic investigations of known events are needed. The 1953 North Sea storm surge was the largest natural disaster for countries bordering the southern North Sea during the twentieth century. We characterize the spatial distribution of a sand deposit from the 1953 storm surge in a salt marsh at Holkham, Norfolk (UK). Radionuclide measurements, core scanning x-ray fluorescence (Itrax), and particle size analyses, were used to date and characterise the deposit. The deposit occurs at the onset of detectable ^{137}Cs - coeval with the first testing of nuclear weapons in the early 1950s. The sand layer is derived from material eroded from beach and dunes on the seaward side of the salt marsh. After the depositional event, accumulation of finer-grained silt and clay materials resumed. This work has important implications for understanding the responses of salt marshes to powerful storms and provides a near-modern analogue of storm surge events for calibration of extreme wave events in the geological record.

1. Introduction

Sea-level rise will be a significant future environmental hazard, with the Intergovernmental Panel on Climate Change projecting that global mean sea level will rise 0.26-0.98 m above present by 2100 (Church et al., 2013). However, the greatest social and economic impacts are when moderate and extreme storms result in coastal flooding, which will increase in frequency with higher sea-levels (Nicholls et al., 2007; Church et al., 2013; Haigh et al., 2016). With the potential for the frequency of storm events to also increase (Seneviratne et al., 2012; Goodwin et al., 2017), it is important to understand how such events may affect emergency response, adaptation and infrastructure planning. There have been recent efforts to increase our understanding of the spatial and temporal clustering of extreme sea-level events, which has implications for the management and repair of flood-defence systems (Haigh et al., 2016). This endeavour requires a comprehensive dataset of extreme events in which to investigate spatial and temporal trends and provide information on coastal resilience and geomorphic response. In the United Kingdom, Haigh et al. (2015, 2017) have developed a database of 329 coastal flood events from 1915 to 2016 (SurgeWatch) based upon a variety of sources. Of these, eight events are ranked as severe and one as disastrous, the latter being the storm surge of 1953.

To be able to better understand these high-impact low-probability events, it is important to have a much larger dataset (greater than the current nine documented events), from which to construct detailed analysis which requires turning to historical (e.g., RMS, 2007) and geological records of extreme sea levels and storm events. Coastal geological archives have provided evidence of hurricane landfall (e.g., van de Plassche et al., 2006; Brandon et al., 2014), as well as European storm surges (e.g., Tsompanoglou et al., 2010; Bateman et al., 2018). However, use of the geological archive in geohazard assessment requires understanding of how such events are preserved in coastal environments. Identification of sedimentary deposits associated with extreme wave events (e.g., tsunamis and storm surges) in the geological record is often difficult (Sedgwick and Davis, 2002; Kortekaas and Dawson, 2007). Even within more recent times there are a paucity of studies and data (e.g., Dawson et al., 1995; Kortekaas and Dawson, 2007). Such geological evidence can aid in detecting past changes in storm surge activity, by extending reconstructions of storm surges from tide gauge records and of storm indices further back in time.

In this paper, we conduct a geological investigation into the preservation of the well-documented 1953 storm in a salt marsh environment, >60 years after the original event. The 1953 storm was the most severe rapid event to occur in the North Sea during the 20th Century. The event occurred when a storm surge from the North Sea swept across the northwest European shelf and flooded low-lying coastal areas of countries around the North Sea. The resulting disaster in terms of loss of life and damage to infrastructure was enormous. The Netherlands was worst affected with 1836 people killed; in the UK and Belgium, death tolls were 307 and 22, respectively (Gerritsen, 2005). The storm surge led to breaches of coastal flood defences and produced the highest still-water levels on record at several tide gauges on the UK east coast. Several features were observed in the coastal zone at the time, including notches in soft rock cliffs, cliff retreat, and erosion of coastal dunes and reactivation of wash-over deposits (Spencer et al., 2015). However, the expression of the 1953 storm surge in the stratigraphic record around the North Sea remains unclear. Many previous studies of extreme wave events in the stratigraphic record have relied on detailed sedimentological descriptions and micropaleontology (e.g., Kortekaas and Dawson, 2007; Morton et al., 2007). Here we combine sedimentology with elemental geochemistry to identify a known event in a salt marsh. In addition, an understanding of the effects of past storm surges (e.g. the December 1981 event in the Severn Estuary; Croudace et al., 2012) is much needed in the UK as future such events may pose a significant threat to existing coastal industrial and urban infrastructure, and planned nuclear reactors on the coast (e.g., Hinkley, Somerset; Sizewell, Suffolk; and Bradwell, Essex).

2. Study site

Our study site is a small salt marsh at Holkham on the north-facing coastline in North Norfolk, UK (52.974532ºN, 0.759193ºE; Figure 1). The salt marsh is located east of the River Burn and behind an extensive coastal dune system. This coastline is low-lying and characterised by a moderate to low wave regime from the North Sea, westerly longshore drift and macro-meso tidal ranges (Andrews et al., 2000; Bateman et al., 2015). The coast at Holkham prograded during the Holocene and there is active accumulation of beach dunes at present (Andrews et al., 2000; Bateman et al., 2018). We targeted Holkham marsh to identify and describe the geological deposit resulting from the North Sea flood of 1953 because the event caused flooding with water reaching up to 6.31 m OD nearby at Wells-Next-The-Sea in Norfolk (Supplementary material 1), erosion of dunes, and deposition of shingle and sand on salt marshes at this location (Steers, 1953; Spencer et al., 2015).

3. Materials and methods

Seventy-six cores were taken across Holkham marsh using gouge and dutch augers to determine the general stratigraphy of the site (Figures 1 and 2). A master core (where the thickest 1953 storm deposit was found) was then collected using a Russian corer following de Vleeschouwer et al. (2010) for further laboratory analyses. Cores were logged in the field following Tröels-Smith (1955) and a subset of cores were surveyed into a local benchmark. The age-depth relationship of the core is based on ^{210}Pb and ^{137}Cs determinations using high-resolution Gamma spectrometry at the GAU-Radioanalytical Unit (National Oceanography Centre in Southampton – NOCS). Samples were prepared and analysed following standard procedures to determine ^{210}Pb content (e.g., through measurement of the granddaughter radionuclide ^{210}Po) and ^{137}Cs activity. Calculation of the sediment accretion rate (SAR) (cm yr^{-1}) assumes that no radionuclide migration occurs within the sediment profile following deposition. However, the post-depositional mobility of the radionuclides and sedimentation phases should be considered during interpretation. The application of ^{210}Pb and ^{137}Cs dating in coarse-grained sediments could also be hindered by the lower sorption capacity of siliceous particles (Tsompanoglou et al., 2010).

XRF geochemical scanning is a time and cost-efficient means to obtain high-resolution geochemical information and laser diffraction particle size analysis can provide detailed information on grain size populations in a sedimentary succession; hence, both methods were used. Itrax X-ray fluorescence core scanning was undertaken at NOCS, using Mo and Cr X-ray tubes. The peak area intervals are “nominally proportional to concentrations of major and minor elements within the sediment” (Croudace et al., 2006). Particle size analysis was carried out using a Coulter LS230 Laser Diffraction Particle Size Analyser following removal of organics using hot H_2O_2. End-member modelling analysis (EMMA) was performed on each grain-size dataset following Dietze et al. (2012). Bulk density and loss-on-ignition were undertaken using standard methods (Chambers et al., 2010). Magnetic susceptibility of the cores was determined using a Bartington loop sensor (MS2C) and MS2 instrument.

4. Results and discussion

The locations of the seventy-six cores in the Holkham marsh are shown in Figure 2. The stratigraphy of the Holkham salt marsh is characterised by clays and silts with organics and occasional sand which is typical of salt marsh environments (Figure 3). A sand horizon was present at ~40-60 cm below the surface in most cores, possibly representing an earlier event than the 1953 storm. At the landward (southern) side of the marsh the uppermost sediment is a peaty soil, reflecting development of high-marsh. Dune sands, sometimes covered with peaty soils, are present in the northern portion of the salt marsh (Figure 3).

In the south-east portion of the marsh (in 16 of the 76 cores) a thin sand layer of between 0.5 and 3.0 cm thick (μ = 1.26 cm) was found between 23 and 28 cm (μ = 25.4 cm) in the cores (Figures 2-4). The altitude of the base of the sand layer varies between 2.5 and 2.7 m above Ordnance Datum (UK) (μ = 2.6 m) (Figure 4). The maximum thickness of the deposit is greatest in the southern landward edge of the marsh which is slightly higher in elevation (Figure 4). There is a significant correlation between elevation of the thin sand deposit where it is present and latitude (r=0.74; p<0.001) suggesting that the topography of the marsh was similar in the past to today (higher in the southern edge). There is no significant relationship between longitude and elevation of the thin sand unit. There is a significant relationship between thickness of the thin sand unit and elevation (r=0.55, p<0.05), illustrating that the thicker units are in the higher southern parts of the marsh.

In the core analysed in detail, profiles of ^{137}Cs and ^{210}Pb show trends associated with changing radionuclide inputs and sediment composition (Figure 5) and produce consistent chronologies. ^{137}Cs variations provide evidence for two main rates of sediment accumulation that are largely corroborated by the ^{210}Pb record (determined by gamma spectrometry). Key markers in the ^{137}Cs record were used to build the age model, including: (1) the first appearance of ^{137}Cs, coincident with the onset of atmospheric nuclear weapons testing ~1954 (range = 1950-1955); (2) the ^{137}Cs bomb peak (1963, albeit rather subtle); and (3) changing inputs from marine discharges from the Sellafield reprocessing plant as revealed by distinct inflections (Gray et al., 1995; Tsompanoglou et al., 2010). McCubbin et al. (2002) estimated solution transport of conservative radionuclides to be approximately two years between Sellafield and East Anglia. However, Shimmield (1997) and Lee and Cundy (2001) suggest 5-8 years for particulate transport and based on this it was decided to apply a 7- year lag for Sellafield inputs to Norfolk salt marshes (Figure 5). This information when incorporated into an age-depth relationship for the Holkham salt marsh (Figure 5) shows good linearity which validates the proposed fit. The ^{137}Cs record reveals two linear SARs (Figure 5). The SAR rate after the 1953 flood is approximately 0.48 cm yr^{-1} which later reduced to approximately 0.28 cm yr^{-1}; and the two rates are seen in both the ^{210}Pb and ^{137}Cs data. Any small signal from the 1986 Chernobyl accident in UK east coast salt marshes is obscured by the signal from the Sellafield discharges (Tsompanoglou et al., 2010).

The thin sand unit was found at 23-26 cm in the analysis core and is composed primarily of medium sand, with D_{90} (the grain size at which 90% of the sample is finer) ranging from 365-500 µm, which is too coarse for dune sand but typical of storm surge deposits (Boldt et al., 2010). The base of the sand unit is tightly constrained to 1950-1955 as it is concomitant with the first detectable ^{137}Cs in the profile, and thus the onset of nuclear weapons testing (Figure 5), signifying that it represents the storm deposit from the 1953 storm surge event. The sand unit is overlain by sediment comprised primarily of poorly-sorted medium silt. Bulk density increases and organic content decreases at 23-26 cm depth, reflecting input of coarse-grained material (> 63 µm) to the marsh and reduction in the accumulation of fine-grained (< 63 µm) material that typifies the rest of the record (Figure 6). The decrease in SAR over time suggests that the marsh is either reaching maturity, accommodation space is being infilled, or that the sedimentation rate has been adversely affected by the deposition of sand during the 1953 storm.

The sand unit dated to the 1953 storm surge event shows a distinct elemental composition: Ca, Cl, K, Rb, Ti, Y decline compared with previous values and Si increases at 23-26 cm (Figures 7 and 8). The study region is underlain by the Newhaven Chalk Formation with abundant clay minerals and calcite cements of variable trace element composition and the Wells Marl that contains up to 10% bentonite. Input of elements from this bedrock and derived surficial sediments are expected to include elements typical of clastic material of crustal origin (e.g, Al, Si, K, Ti, Fe, and Rb; Mügler et al., 2010) in addition to other elements commonly associated with clay minerals (e.g., Ba, Ca, Mg, Mn, Na, V, and Zn) and calcite cements (e.g., Sr). Zirconium and Si are also commonly associated with medium to coarse grain-sized clastic material (Koinig et al., 2003; Kylander et al., 2011; Haenssler et al., 2014). During the 1953 storm surge event, a decline in Fe, Cl, K, Rb, and Ti occurs in the chemostratigraphic record of Holkham Marsh, concurrent with an increase in Si that reflects the geologically instantaneous input of coarse-grained detrital material that diluted both organic matter deposition and the input of materials derived from catchment geology (Koinig et al., 2003; Kylander et al., 2011; Jeans et al., 2014) (Figures 7 and 8). While the majority of Si is likely derived from aluminosilicate minerals, this element can also represent a biogenic component (e.g., diatom frustules; Kylander et al., 2011).

Changes are also reflected by variations in the Ca/K and Ca/Ti ratios driven by a decline in K and Ti relative to Ca in the 1953 sand horizon (Figures 7 and 8). Sedimentary Ca can be autochthonously derived through carbonate precipitation in saturated waters during summer months, but its decline during the 1953 storm surge event suggests the majority of Ca is derived from weathering in the catchment (Cohen, 2003; Haenssler et al., 2014).

Increases in the concentration of Na, SO_4^{2-}, Cl, Ca, and Mg have been previously documented in washover deposits attributed to tsunamis in New Zealand (Chague-Goff and Goff, 1999; Goff and Chague-Goff, 1999; Chague-Goff et al., 2000; Goff et al., 2001). Storm surge deposits, in contrast, transport sediment inland from nearshore and beach environments. Differences in sediment source of storm surge deposits vs. tsunami explain the Si-dominated signature observed in the 1953 storm surge deposit at Holkham. End-Member Mixing Analysis (EMMA) identified two robust end members within the whole-core particle size data (For full method see Supplementary material 2). The first end member has a mode of 14.96 mm (poorly-sorted medium silt) and the second end member (EM02:

the storm deposit) has a mode of 324.7 mm (well-sorted medium sand). EM02 is first observed in the 25-26 cm interval and is composed of both end-members in equal proportions. The 24-25 cm interval is composed solely of EM02 (324.7 µm) and is the last interval to host EM02. The 24 to 25 cm interval is composed solely of EM02 (324.7 µm) and is the last interval to host EM02. The EMMA analysis provides a means to differentiate storm surge from tsunami deposits; storm deposits have unimodal large particle size distribution indicating unidirectional sediment transport. In contrast, backwash associated with tsunami results in a second, coarser, sediment population (Goff et al., 2001, 2004). Tsunami deposits are also usually characterised by several discrete wave events, with several fining-up sequences in stratigraphic records (Smith, 2005).

The position of the preserved storm deposits indicates that the dunes may have been breached by the storm surge at the point where the causeway and path cross through the low point in the dunes to the north-east of the marsh (Figure 2), where a potential small washover fan is observed encroaching onto the marsh. The storm surge would have entrained both dune and beach sand as it overtopped the dunes at the low point. As the surge then diffracted into the marsh behind, it deposited fine dune and medium beach sand over the eastern side of the marsh. The initial north-east to south-west surge wave may have deposited sand across the entire eastern side of the marsh, but its preservation is greatest on the north-eastern margins of tidal creek channels. After initial diffraction, the storm surge may have reflected off the causeway embankment at the landward side of the marsh, creating localised backwash. This lower-energy backwash would have travelled generally north-east, potentially remobilising some of the sand on the southern margins of the channels and removing it from the marsh through the tidal creek network. This would account for the observed patchy preservation of the sand. However, whether there was a single, large surge wave or repeated waves overtopping the barrier is unknown, as repeated waves would also have the potential to cause remobilisation. Preservation of sediments associated with extreme events may also be focused in surface depressions, having been removed from topographic highs (Engel and Brückner, 2011).

Our findings differ from those obtained by Tsompanoglou et al. (2010) from a salt marsh on the northern shore of The Wash embayment, to the north of our study site. In that study the 1953 storm surge event is manifested as a thin silty sand layer as the salt marsh was partly eroded and heavy-mineral-enriched grains settled on the erosion salt marsh platform, creating a distinctive horizon. During the 1953 storm a 2-m high surge (excluding waves) was recorded in The Wash and off the North Norfolk coast (Robinson, 1953; Environment Agency, 2015). At Holkham, sand was rapidly eroded from beach and/or dune sands during the 1953 storm and deposited across the marsh surface (Figure 1). This occurred in sufficient water depth/energy for sand particles to be transported and deposited. There is documentary evidence of flooding of reclaimed marshes, breaches of flood defences, erosion of dunes, and most importantly in this case the washing of shingle and sand onto marshes at Holkham (Steers, 1953). Following the deposition of sand, salt marsh accumulation continued with typical finer-grained material, indicating a return to regular salt marsh sedimentation. At Holkham, the depositional setting was not permanently affected and following the storm event 'typical' sedimentation resumed albeit at a slower rate.

In the geological record, storm surge deposits may be differentiated from other extreme wave events (e.g., tsunamis) by several sedimentological features associated with differences in hydrodynamics and sediment-sorting processes (Kortekaas, 2002). Storm surges have lower shear stress than tsunamis, resulting in less or no erosion inland, are manifested at the shore by repeated inundation by short-wavelength, short-period storm waves that erode the shoreface and transport those sediments inland, and have many small, short-period waves of uni-directional inundation (Switzer and Jones, 2008). As a result, storm surge deposits can be distinguished from tsunami deposits by the absence of mud intraclasts, unidirectional imbrication if present, and unimodal coarse grain size signatures (Kortekaas, 2002; Engel and Bruckner, 2011). Sediment transport associated with storm surges is mainly by traction with minimal suspension (Morton et al., 2007) and the resulting deposits are composed of sub-horizontal planar laminae that are often graded and derived from the proximal nearshore and beach face (Kortekaas, 2002; Switzer and Jones, 2008). While tsunami deposits tend to be < 25 cm, sandy storm deposits are larger, generally >30 cm (e.g., Switzer and Jones, 2008). The sand deposit preserved in Holkham is, in contrast, only ~3 cm thick, and has no visual sedimentary features. This difference in thickness may be due to i) the 1953 storm surge being small than the events identified in the geological record; ii) erosion of the original deposit at Holkham; iii) a relatively small volume of sediment was delivered to the marsh in 1953; iv) differences in accommodation space; and v) a bias of only recording thicker storm surge deposits in the geological record.

Our results provide an example of identification of a relatively small storm surge deposit using rapid cost-efficient techniques that may be applied to the geological record. The 1953 storm event is not unique in the history of Norfolk with other storms recorded after (e.g., 1978 and 2013) and before (e.g., 1903 and 1853). There is the possibility that the less extreme 1978 storm is also preserved in our core as an increase in bulk density and decrease in organic matter, although there is no visually identifiable sand layer (Figure 6). The lower sand unit at Holkham (~40-60cm depth) may represent an earlier storm event.

Applying the above methodologies to this salt marsh record demonstrates the potential to provide detail on the magnitude and extent of the impacts of the past storms and also to extend the record to events prior to the documentary period. Such information could make an important contribution to debates concerning the changing frequency of storms within the North Sea (e.g., Dangendorf et al., 2014) and also the magnitude and return intervals of storm surges for coastal zone risk management. The patchy preservation of the 1953 storm sand also highlights the uncertainty in preservation and correlation of high-energy event deposits over a longer-term geological record, and that even well-constrained events may be highly localised in their geological expression. We show that the 1953 storm event is preserved in a small landward pocket of a Norfolk salt marsh, which could easily have been missed during coring investigations elsewhere on this marsh. This study demonstrates that it is important to consider the path of the event waves which transport material onto a marsh. Future studies of palaeo storm surge deposits should target locations where an abundant supply of nearby mobile sediment could easily have accumulated and not be eroded by subsequent backwash through the local tidal creek network. Finding such environments may not be possible in some locations, so it is also important to consider the lack of preservation of sediments associated with extreme coastal events when using such data for geohazard assessment.

5. Conclusions

We identify a fine to coarse-grained sand deposit in a salt marsh at Holkham, Norfolk, UK and use ^{137}Cs dating to constrain it to the early 1950s. We contend that the deposit was derived from an extreme wave event associated with the 1953 North Sea storm surge – the most severe rapid event to occur in the North Sea during the 20th century. The sand unit is derived from material eroded from beach and dune sands on the seaward side of the salt marsh and is geochemically distinct by an increase in Si. The rapid deposition of the sands diluted the background detrital input of aluminosilicates derived from bedrock and derived surficial materials. After the deposition event, accumulation of finer-grained silt and clay material resumed. The sedimentary record of the 1953 event is relatively patchy in this location. It is important to consider the potential surge pathway, the availability of local mobile sediment and the nature of the local depositional environment when considering where might best preserve records of multiple historic storm surges. Our results i) have important implications for how geological archives of coastal geohazards may be interpreted where there is an absence of historical archives; ii) improve the understanding of the response of low-lying coastal marshes to storm surges; and iii) clarify how storm surge deposits can be identified in the stratigraphic record using this near-modern analogue.

Acknowledgements

We thank the White Rose Collaboration Fund for funding this work. We also gratefully acknowledge the use of facilities at NOC, Southampton (BOSCORF Itrax) and the University of Southampton

(GAU Radiometric Dating Laboratories). Sarah Henderson and the Holkham Estate are thanked for their assistance in working at Holkham. GR was funded by a NERC doctoral training grant (NE/L002450/1). This paper represents NRCan contribution number 20180084 (JMG).

Figure captions

Figure 1. (a) Map of study site including location of the analysis core. (b) Photograph of the analysis core (showing the 3-cm thick sand unit) from the 1953 storm.

Figure 2. Maps showing the spatial distribution of the 1953 storm deposit at Holkham. Aerial photograph of the salt marsh showing the distribution of the 1953 storm sand layers within the acquired cores (top). The core transect in Figure 3 is shown (black line – cores 1-13). Image copyright Getmapping Plc. 25cm elevation-coloured and hillshaded Digital Terrain Model of Holkham Marsh (bottom). The thickness of the 1953 storm sand deposit encountered within each core is shown. The suggested pathway of the 1953 storm wave is illustrated as a dashed arrow. Contains public sector information (25cm LiDAR, copyright Environment Agency) licensed under the UK Open Government Licence v 3.0.

Figure 3. Lithostratigraphic transect of Holkham salt marsh (core 1-13 locations are shown in Figure 2). The height of the marsh surface, based on a Digital Terrain Model (Figure 2) is also illustrated (m above Ordnance Datum).

Figure 4. (a) Histogram showing the variation in thickness of the 1953 storm layer (a kernel density function is shown). (b) Graph showing thickness of the 1953 storm against elevation of the bottom of the layer. A linear least-squares regression line and 95% confidence limits are shown. (c) Spatial interpolation plot of 1953 layer thickness. A thin-plate spline was used as the interpolation algorithm. The 1953 layer was not found outside of the region shown.

Figure 5. Chronological information for the Holkham core: (a) ^{210}Pb data with logarithmic trend lines (orange = faster post-surge SAR and blue = slower, more recent SAR;); (b) ^{137}Cs profile annotated

with key chronological markers taken from the Sellafield temporal discharge profile with a lag of 7-years added to the features; (c) age-model based on linear regression suggesting a change in sediment accumulation rate; and (d) Sellafield ^{137}Cs temporal discharge profile around Irish Sea (Gray et al., 1995).

Figure 6. Physical and sedimentological properties of the Holkham marsh core. The 1953 storm deposit horizon is illustrated. The potential horizon of the 1978 storm is also shown.

Figure 7. Summary XRF analysis (lithophile elements). The 1953 storm horizon is illustrated.

Figure 8. Elemental profiles from Itrax analysis. The 1953 storm horizon is illustrated.

References

Andrews, J.E., Boomer, I., Bailiff, I., Balson, P., Bristow, C., Chroston, P.N., Funnell, B.M., Harwood, G.M., Jones, R., Maher, B.A., Shimmield, G.B., 2000. Sedimentary evolution of the north Norfolk barrier coastline in the context of Holocene sea-level change, in Shennan, I., Andrews, J., eds., Holocene Land-ocean Interaction and Environmental Change Around the North Sea, Geological Society, London, Special Publication 166, 219–251.

Bateman, M.D., Stein, S., Ashurst, R. A., Selby, K., 2015. Instant luminescence chronologies? High resolution luminescence profiles using a portable luminescence reader. Quaternary Geochronology 30B, 141–146.

Bateman, M.D., Rushby, G. Stein, S., Ashurst, R.A. Stevenson, D., Jones, J.M. Gehrels, W.R., 2018. Can sand dunes be used to study historic storm events? Earth Surface Processes and Landforms (in press). https://doi.org/10.1002/esp.4255.

Boldt, K.V., Lane, P., Woodruff, J. D., Donnelly, J.P., 2010. Calibrating a sedimentary record of overwash from Southeastern New England using modelled historic hurricane surges. Marine Geology 275, 127–139.

Boyle, J.F., 2001. Inorganic geochemical methods in paleolimnology, in Last, W.M., and Smol, J.P., eds., Tracking Environmental Change Using Lake Sediments, Vol. 2, Physical and Geochemical Methods, Kluwer Academic Publishers, Dordrecht, 83–142.

Brandon, C.M., Woodruff, J.D., Donnelly, J.P., Sullivan, R.M., 2014. How unique was Hurricane Sandy? Sedimentary reconstructions of extreme flooding from New York Harbor. Scientific Reports 4, 7366.

Chague-Goff, C., Goff, J., 1999. Geochemical and sedimentological signature of catastrophic saltwater inundations tsunami, New Zealand. Quaternary Australasia 17, 38–48.

Chague-Goff, C., Nichol, S.L., Jenkinson, A.V., Heijnis, H., 2000, Signatures of natural catastrophic events and anthropogenic impact in an estuarine environment, New Zealand. Marine Geology 167, 285–301.

Chambers, F.M., Beilman, D.W., Yu, Z. 2010. Methods for determining peat humification and for quantifying peat bulk density, organic matter and carbon content for palaeostudies of climate and peatland carbon dynamics. Mires and Peat 7, 10pp. http://mires-and-peat.net/pages/volumes/map07/map0707.php

Church, J.A., Clark, P.U., Cazenave, A., Gregory, J.M., Jevrejeva, S., Levermann, A., Merrifield, M.A., Milne, G.A., Nerem, R.S., Nunn, P.D., Payne, A.J., Pfeffer, W.T., Stammer, D., Unnikrishnan, A.S., 2013. Sea Level Change, in: Stocker, T.F., Qin, D., Plattner, G.-K., Tignor, M., Allen, S.K., Boschung, J., Nauels, A., Xia, Y., Bex, V., Midgley, P.M. (Eds.), Climate Change 2013: The Physical Science Basis. Contribution of Working Group I to the Fifth Assessment Report of the Intergovernmental Panel on Climate Change. Cambridge University Press, Cambridge, United Kingdom and New York, NY, USA, pp. 1137–1216.

Cohen, A.S., 2003. Paleolimnology. The History and Evolution of Lake Systems: Oxford University Press, Oxford.

Croudace, I.W., Rindby, A. and Rothwell, R.G., 2006. ITRAX: Description and evaluation of a new sediment core scanner *in* R.G. Rothwell *(ed.). New techniques in sediment core analysis.* Geol. Soc. Spec. Publ., 267, 51–63.

Croudace, I.W., Warwick, P.E., Morris, J.E., 2012. Evidence for the preservation of technogenic tritiated organic compounds in an estuarine sedimentary environment. Environ. Sci. Technol. 46, 5704–5712.

Dangendorf, S., Mueller-Navarra, S., Jensen, J., Schenk, F., Wahl, T., Weisse, R., 2014. North Sea storminess from a novel storm surge record since AD 1843. Journal of Climate 27, 3582–3595.

Dawson, A.G., Hindson, R., Andrade, C., Freitas, C., Parish, R., Bateman, M., 1995. Tsunami sedimentation associated with the Lisbon earthquake of 1st November AD 1755: Boca Do Rio, Algarve, Portugal. The Holocene 5, 209–215.

De Vleeschouwer, F., Chambers, F.M., Swindles, G.T., 2010. Coring and sub-sampling of peatlands for palaeoenvironmental research. Mires and Peat 7, Article 1, 1–10.

Dietze, E., Hartmann, K., Diekmann, B., IJmker, J., Lehmkuhl, F., Opitz, S., Stauch, G., Wünnemann, B., Borchers, A., 2012. An end-member algorithm for deciphering modern detrital processes from lake sediments of Lake Donggi Cona, NE Tibetan Plateau, China. Sedimentary Geology 243-244, 149–180.

Engel, M., and Brückner, H., 2011. The identification of palaeo-tsunami deposits – A major challenge in coastal sedimentary research. Coastline Reports 17, 65–80.

Environment Agency, 2015. https://www.gov.uk/government/organisations/environment-agency

Gerritsen, H., 2005. What happened in 1953? The Big Flood in the Netherlands in retrospect. Phil. Trans. R. Soc. A 363, 1271–1291.

Goff, J.R., Chague-Goff, C., 1999. A late Holocene record of environmental changes from coastal wetlands: Abel Tasman National Park, New Zealand. Quaternary International 56, 39–51.

Goff, J.R., Chague-Goff, C., Nichol, S., 2001. Palaeotsunami deposits: a New Zealand perspective. Sedimentary Geology 143, 1–6.

Gray, J., Jones, S.R., Smith, A.D., 1995. Discharges to the environment from the Sellafield site, 1951-1992. J. Radiol. Prot. 15**,** 99–131.

Goodwin, P., Haigh, I.D., Rohling, E.J., Slangen, A., 2017. A new approach to projecting 21st century sea-level changes and extremes. Earth's Future 5, 240–253.

Haenssler, E., Unkel, I., Dörfler, W., Nadeau, M-J., 2014. Driving mechanisms of Holocene lagoon development and barrier accretion in Northern Elis, Peloponnese, inferred from the sedimentary record of the Kotychi Lagoon. E&G Quaternary Science Journal 63, 60–77.

Haigh, I.D., Ozsoy, O., Wadey, M.P., Nicholls, R.J., Gallop, S.L., Wahl, T., Brown, J.M., 2017. An improved database of coastal flooding in the United Kingdom from 1915 to 2016. Scientific Data 4, 170100.

Haigh, I.D., Wadey, M.P., Gallop, S.L., Loehr, H., Nicholls, R.J., Horsburgh, K., Brown, J.M., Bradshaw, E., 2015. A user-friendly database of coastal flooding in the United Kingdom from 1915–2014. Scientific data 2, 150021.

Haigh, I.D., Wadey, M.P., Wahl, T., Ozsoy, O., Nicholls, R.J., Brown, J.M., Horsburgh, K., Gouldby, B., 2016. Spatial and temporal analysis of extreme sea level and storm surge events around the coastline of the UK. Scientific Data 3, 160107.

Jeans, C.V., Tosca, N.J., Hu, X.R., Boreham, S., 2014. Clay mineral-grain size-calcite cement relationships in the Upper Cretaceous Chalk, UK: A preliminary investigation. Clay Minerals 49, 299–325.

Koinig, K.A., Shotyk, W., Lotter, A.F., Ohlendorf, C., Sturm, S., 2003. 9000 years of geochemical evolution of lithogenic major and trace elements in the sediment of an alpine lake: the role of climate, vegetation, and land-use history. Journal of Paleolimnology 30, 307–320.

Kortekaas, S., 2002. Tsunamis, storms and earthquakes: distinguishing coastal flooding events. PhD-thesis Coventry University, UK. 171p.

Kortekaas, S., Dawson, A.G., 2007. Distinguishing tsunami and storm depostis: an example from Martinhal, SW Portugal. Sedimentary Geology 200, 208–221.

Kylander, M.E., Ampel, L., Veres, D., Wohlfarth, B., 2011. High-Resolution XRF Core Scanning Analysis of Les Echtes (France) Sedimentary Sequence: New Insights from Chemical Proxies. Journal of Quaternary Science 26, 109–117.

Lee, S.V., Cundy, A.B., 2001. Heavy metal contamination and mixing processes in sediments from the Humber Estuary, Eastern England. Estuarine, Coastal and Shelf Science 53, 619–636.

McCubbin, D., Leonard, K.S., Brown, J., Kershaw, P.J., Bonfield, R.A., Peak, T., 2002. Further studies of the distribution of Technetium-99 and Cesium-137 in UK and European coastal waters. Continental Shelf Research 22, 1417–1445.

Morton, R.A., Gelfenbaum, G., Jaffe, B.E., 2007. Physical criteria for distinguishing sandy tsunami and storm deposits using modern examples. Sedimentary Geology 200, 184–207.

Mügler, I., Gleixner, G., Günther, F., Mäusbacher, R., Daut, G., Schütt. B., Berking, J., Schwalb, A., Schwark, L., Xu, B., Yao, T., Zhu, L., Yi, C., 2010. A multi-proxy approach to reconstruct hydrological changes and Holocene climate development of Nam Co, Central Tibet. Journal of Paleolimnology 43, 625–648.

Nicholls, R.J., Wong, P.P., Burkett, V.R., Codignotto, J.O., Hay, J.E., McLean, R.F., Ragoonaden, R.F., Woodroffe, C.D., 2007. Coastal systems and low-lying areas, in Parry, M.L., Canziani, O.F., Palutikof, J.P., van der Linden, P.J., Hanson, C.E., eds., Climate Change 2007: Impacts, Adaptation and Vulnerability. Contribution of Working Group II to the Fourth Assessment Report of the Intergovernmental Panel on Climate Change, Cambridge University Press, Cambridge, UK, p. 315–356.

RMS, 2007. 1607 Bristol Channel Floods: 400-year Retrospective Report RMS special report.

Robinson A.H.W., 1953. The storm surge of 31 Jan–1 Feb. 1953 and the associated meteorological and tidal conditions. Geography 3, 307–321.

Schofield, J.E., Edwards, K.J., Mighall, T.M., Martínez Cortizas, A., Rodríguez-Racedo, J., Cook, G., 2010. An integrated geochemical and palynological study of human impacts, soil erosion and storminess from southern Greenland since c. AD 1000. Palaeogeography, Palaeoclimatology, Palaeoecology 295, 19–30.

Sedgwick, P.E., Davis, R.A., 2003. Stratigraphy of washover deposits in Florida: implications for recognition in the stratigraphic record. Marine Geology 200, 31–48.

Seneviratne, S., Nicholls, N., Easterling, D., Goodess, C., Kanae, S., Kossin, J., Luo, Y., Marengo, J., McInnes, K., Rahimi, M., 2012. Managing the risks of extreme events and disasters to advance climate change adaptation a special report of Working Groups I and II of the Intergovernmental Panel on Climate Change (IPCC). Cambridge: Cambridge University Press.

Shimmield, G. 1997., The use of radionuclides in assessing salt marsh accretion rates and relative sea-level change. In (Barrett, R.L., ed.). LOIS-Second Annual General Meeting (Abstract), 18–20 March 1997, University of Hull, NERC, Swindon (LOIS publication 323).

Smith, D., 2005. Tsunami: a research perspective. Geology Today 21, 64-68. doi:10.1111/j.1365-2451.2005.00501.x

Spencer, T., Brooks, S.M., Evans, B.R., Tempest, J.A., Möller, I., 2015. Southern North Sea storm surge event of 5 December 2013: Water levels, waves and coastal impacts. Earth Science Reviews 146, 120–145.

Steers, J.A., Stoddart, D.R., Bayliss-Smith, T.P., Spencer, T., Durbidge, P.M., 1979. The storm surge of 11 January 1978 on the east coast of England. The Geographical Journal 145, 192–205.

Switzer, A.D., Jones, B.G., 2008. Large-scale washover sedimentation in a freshwater lagoon from the southeast Australian coast: sea-level change, tsunami or exceptionally large storm? The Holocene 18, 787–1016.

Tsompanoglou, K., Croudace, I.W., Birch, H., Collins, M., 2010. Geochemical and radiochronological evidence of North Sea storm surges in salt marsh cores from The Wash embayment (UK). The Holocene 21, 225–236.

van de Plassche, O., Erkens, G., van Vliet, F., Brandsma, J., van der Borg, K., de Jong, A.F.M., 2006. Salt-marsh erosion associated with hurricane landfall in southern New England in the fifteenth and seventeenth centuries. Geology 34, 829–832.

Highlights

- The expression of storm events in the geological record is poorly understood
- The 1953 North Sea storm surge caused a major natural disaster in the twentieth century
- We describe a sand deposit from the 1953 storm surge in a UK salt marsh
- Our work has implications for understanding salt marsh response to storm events
- We provide a near-modern analogue for extreme wave events in the geological record

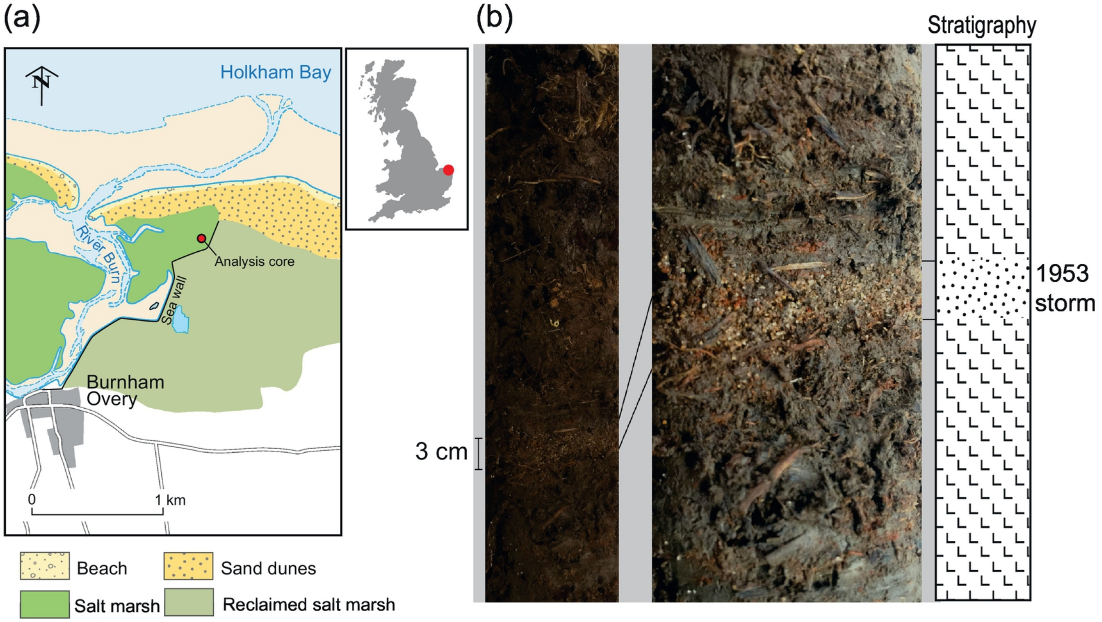
(a)
Holkham Bay
N
River Burn
Analysis core
Sea wall
Burnham
Overy
0
1 km
Beach
Sand dunes
Salt marsh
Reclaimed salt marsh
(b)
Stratigraphy
1953
storm
3 cm

Figure 1

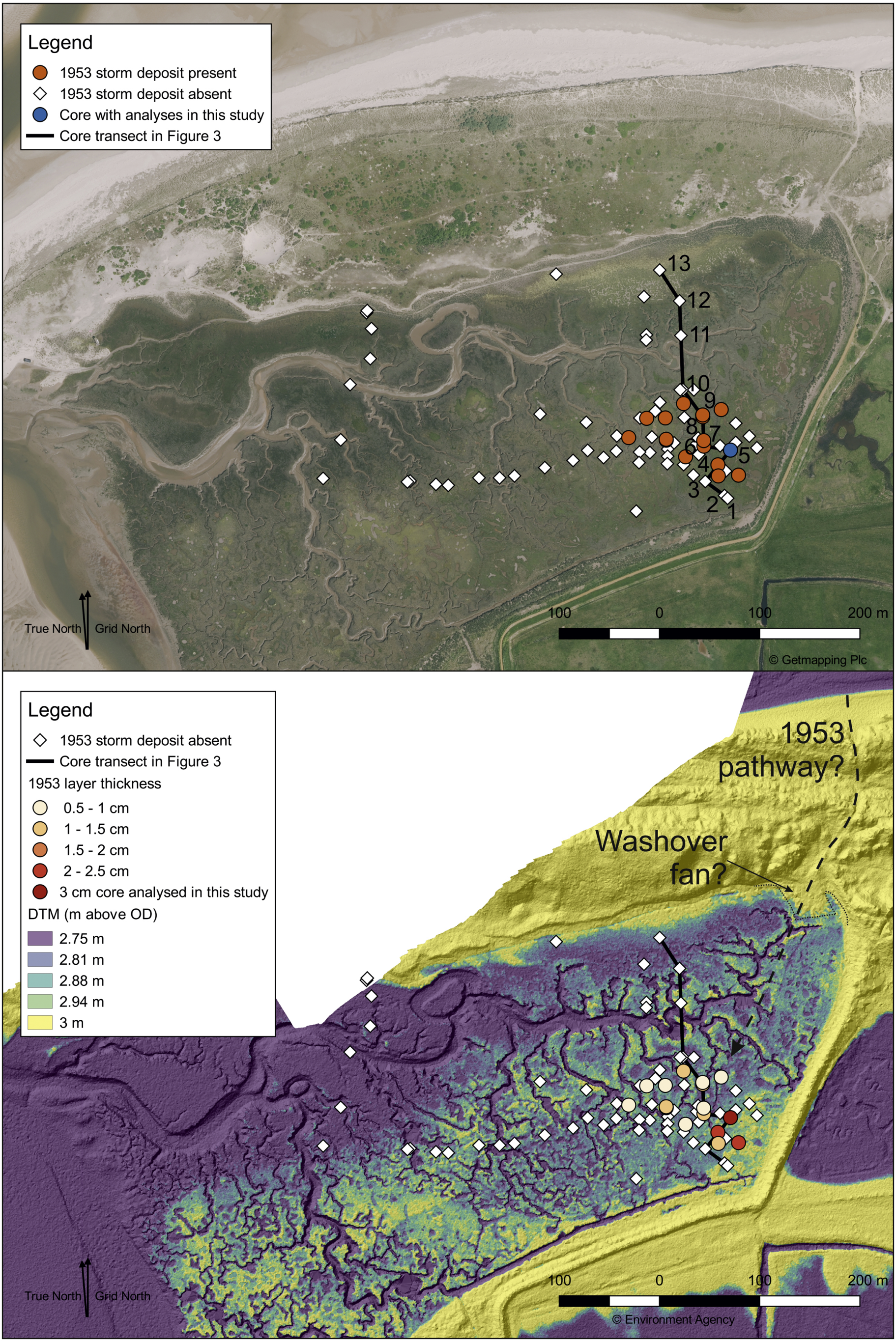
Legend
1953 storm deposit present
1953 storm deposit absent
Core with analyses in this study
Core transect in Figure 3
13
12
11
10
9
8
7
6
5
4
3
2
1
True North
Grid North
100
0
100
200 m
© Getmapping Plc
Legend
1953 storm deposit absent
Core transect in Figure 3
1953 layer thickness
0.5 - 1 cm
1 - 1.5 cm
1.5 - 2 cm
2 - 2.5 cm
3 cm core analysed in this study
DTM (m above OD)
2.75 m
2.81 m
2.88 m
2.94 m
3 m
1953 pathway?
Washover fan?
True North
Grid North
100
0
100
200 m
© Environment Agency

Figure 2

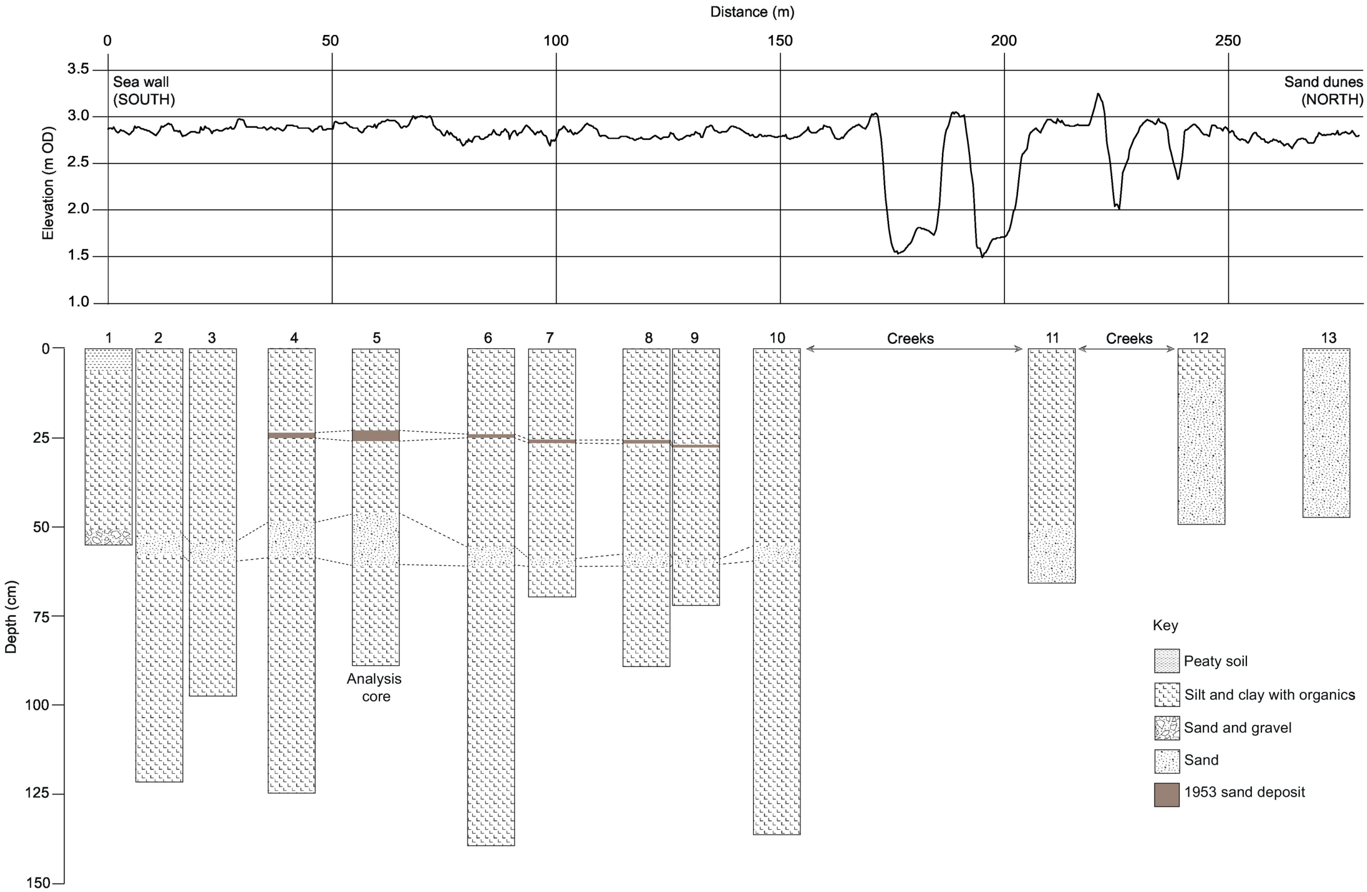
Distance (m)
0
50
100
150
200
250
3.5
3.0
2.5
2.0
1.5
1.0
Elevation (m OD)
Sea wall
(SOUTH)
Sand dunes
(NORTH)
1
2
3
4
5
6
7
8
9
10
Creeks
11
Creeks
12
13
0
25
50
75
100
125
150
Depth (cm)
Analysis
core
Key
Peaty soil
Silt and clay with organics
Sand and gravel
Sand
1953 sand deposit

Figure 3

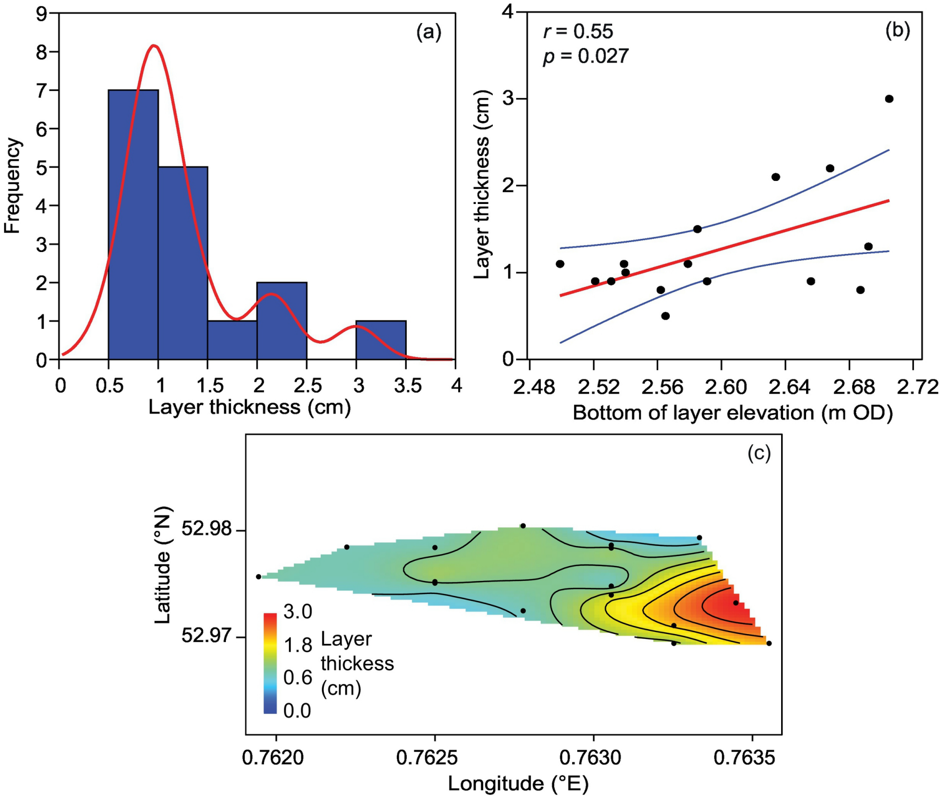
(a)
Frequency
Layer thickness (cm)
0
1
2
3
4
5
6
7
8
9
0.5
1.5
2.5
3.5
(b)
r = 0.55
p = 0.027
Layer thickness (cm)
Bottom of layer elevation (m OD)
2.48
2.52
2.56
2.60
2.64
2.68
2.72
(c)
Latitude (°N)
52.98
52.97
3.0
1.8
0.6
0.0
Layer thickness (cm)
0.7620
0.7625
0.7630
0.7635
Longitude (°E)

Figure 4

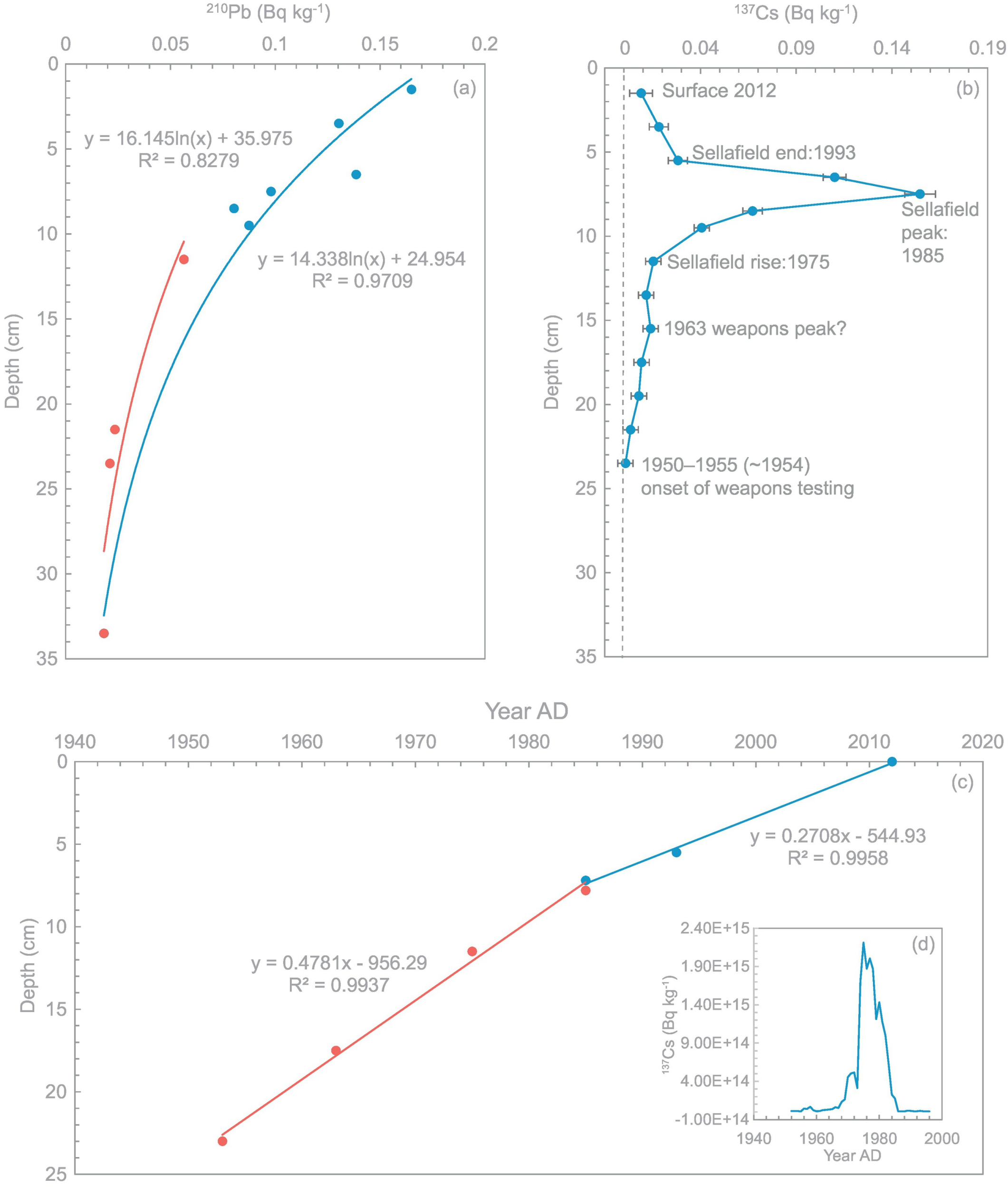

^{210}Pb (Bq kg^{-1})
(a)
y = 16.145ln(x) + 35.975
R² = 0.8279
y = 14.338ln(x) + 24.954
R² = 0.9709
Depth (cm)
^{137}Cs (Bq kg^{-1})
(b)
Surface 2012
Sellafield end:1993
Sellafield peak: 1985
Sellafield rise:1975
1963 weapons peak?
1950–1955 (~1954) onset of weapons testing
Depth (cm)
Year AD
(c)
y = 0.2708x - 544.93
R² = 0.9958
y = 0.4781x - 956.29
R² = 0.9937
Depth (cm)
(d)
^{137}Cs (Bq kg^{-1})
Year AD

Figure 5

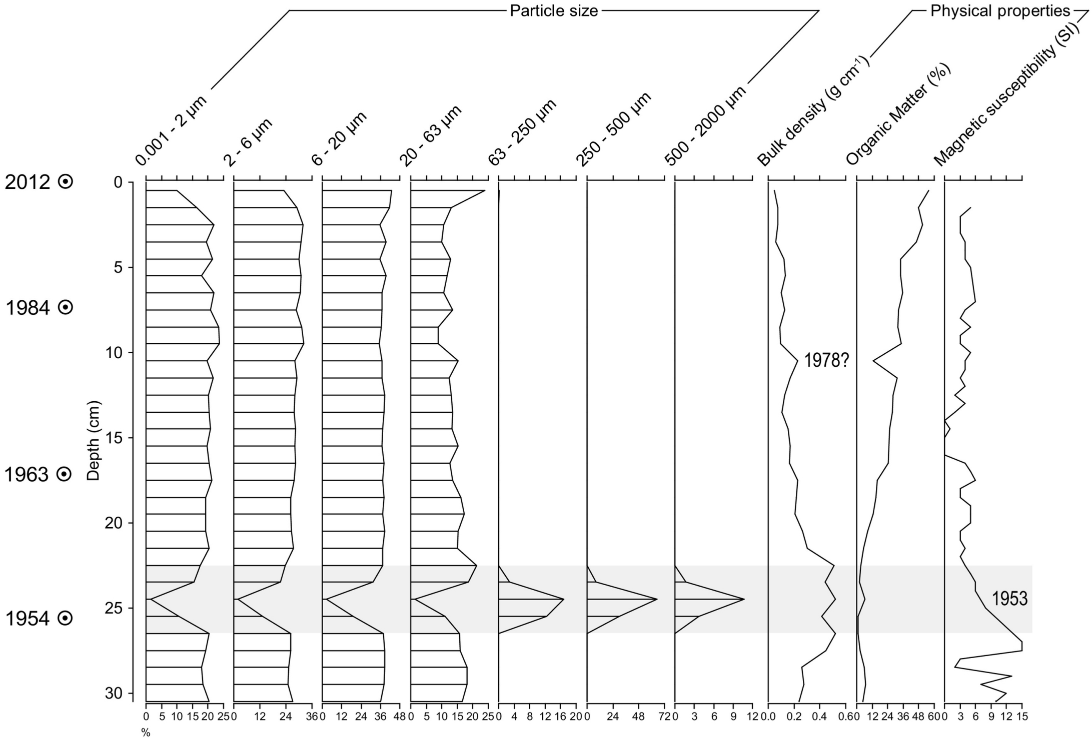
Particle size
Physical properties
0.001 - 2 µm
2 - 6 µm
6 - 20 µm
20 - 63 µm
63 - 250 µm
250 - 500 µm
500 - 2000 µm
Bulk density (g cm-1)
Organic Matter (%)
Magnetic susceptibility (SI)
2012
1984
1963
1954
Depth (cm)
1978?
1953
%

Figure 6

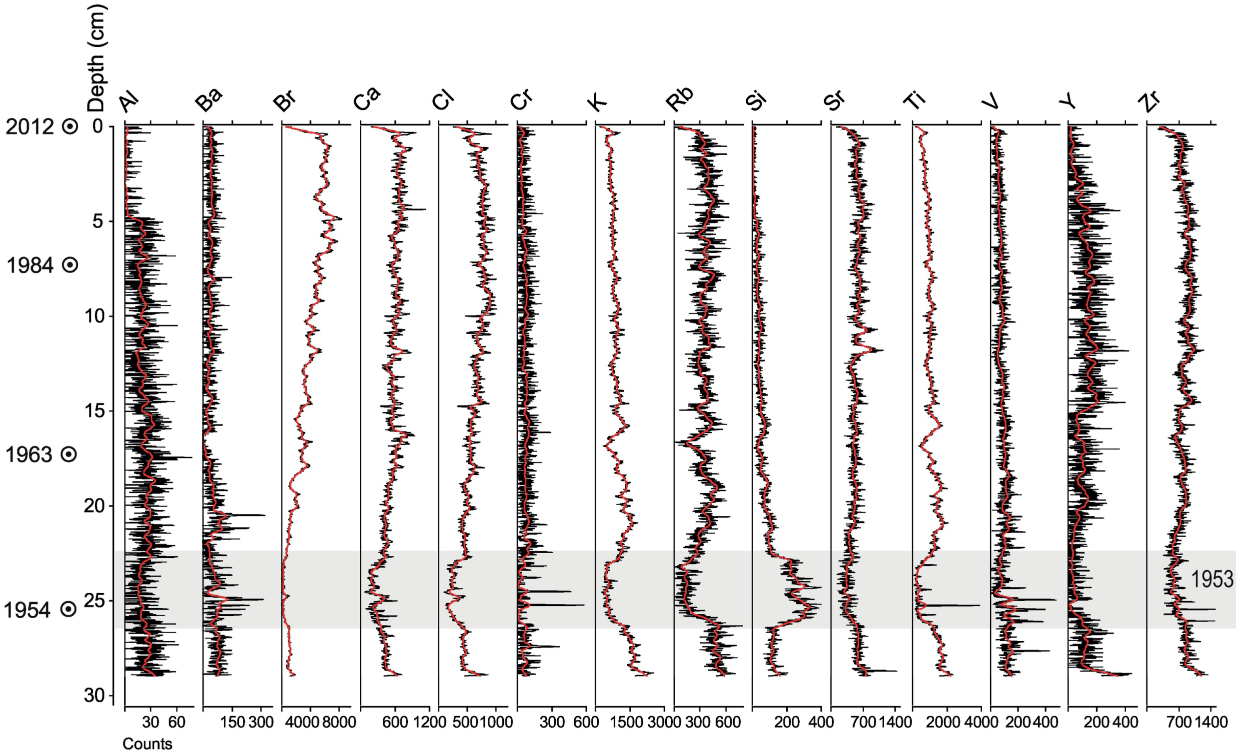
Depth (cm)
Al
Ba
Br
Ca
Cl
Cr
K
Rb
Si
Sr
Ti
V
Y
Zr
2012
1984
1963
1954
1953
0
5
10
15
20
25
30
30 60
150 300
4000 8000
600 1200
500 1000
300 600
1500 3000
300 600
200 400
700 1400
2000 4000
200 400
200 400
700 1400
Counts

Figure 7

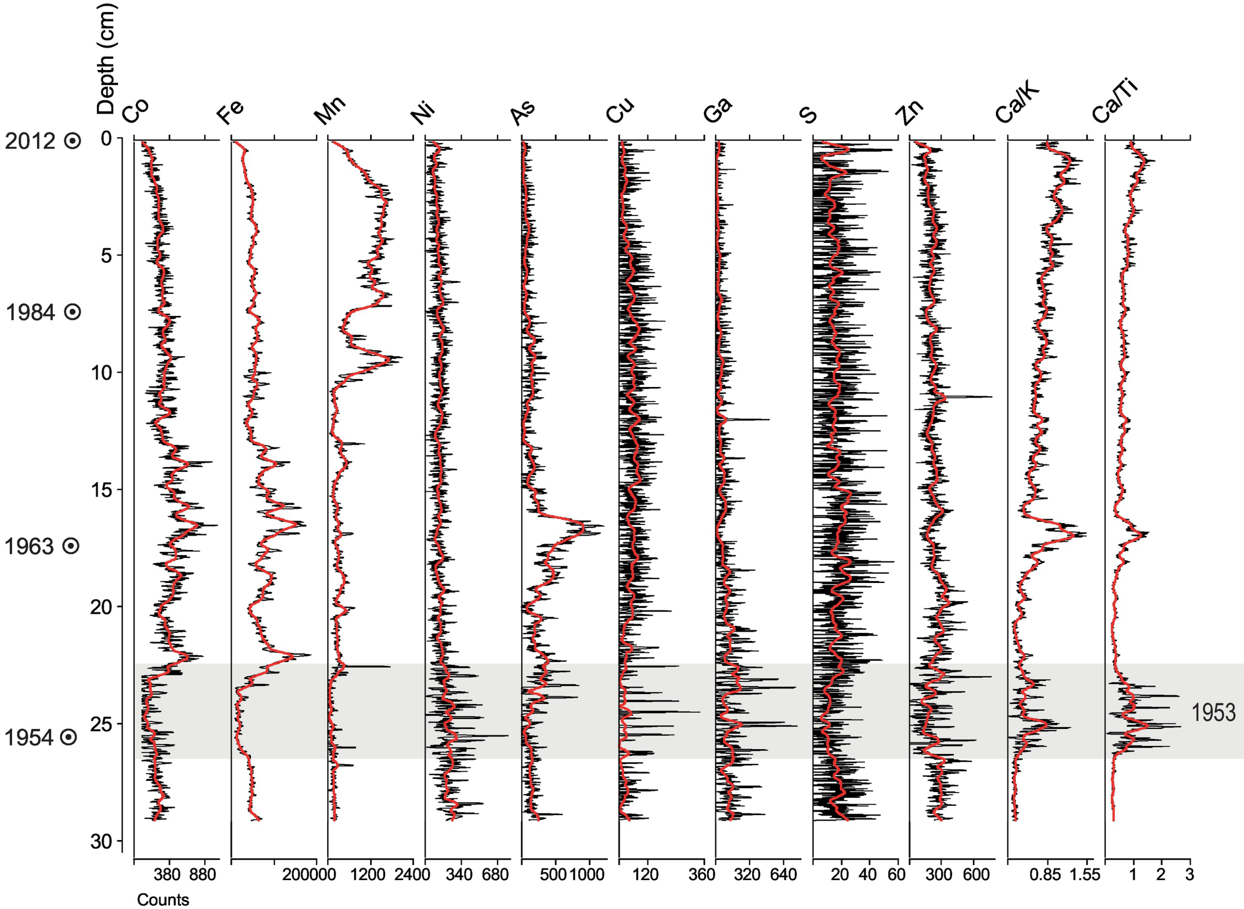
Depth (cm)
Co
Fe
Mn
Ni
As
Cu
Ga
S
Zn
Ca/K
Ca/Ti
2012
1984
1963
1954
1953
0
5
10
15
20
25
30
380 880
Counts
200000
0 1200 2400
340 680
500 1000
120 360
320 640
20 40 60
300 600
0.85 1.55
1 2 3

Figure 8